

Mean-field closure parameters for passive scalar turbulence

This article has been downloaded from IOPscience. Please scroll down to see the full text article.

2012 Phys. Scr. 86 018406

(<http://iopscience.iop.org/1402-4896/86/1/018406>)

View [the table of contents for this issue](#), or go to the [journal homepage](#) for more

Download details:

IP Address: 130.225.213.198

The article was downloaded on 06/07/2012 at 20:26

Please note that [terms and conditions apply](#).

Mean-field closure parameters for passive scalar turbulence

J E Snellman^{1,2}, M Rheinhardt^{1,2}, P J Käpylä^{1,2}, M J Mantere^{1,2}
and A Brandenburg^{2,3}

¹ Department of Physics, Gustaf Hällströmin katu 2a, PO Box 64, FI-00014 University of Helsinki, Finland

² NORDITA, Royal Institute of Technology and Stockholm University, Roslagstullsbacken 23, SE-10691 Stockholm, Sweden

³ Department of Astronomy, Stockholm University, SE-10691 Stockholm, Sweden

E-mail: jan.snellman@helsinki.fi

Received 20 December 2011

Accepted for publication 13 March 2012

Published 4 July 2012

Online at stacks.iop.org/PhysScr/86/018406

Abstract

Direct numerical simulations (DNSs) of isotropically forced homogeneous stationary turbulence with an imposed passive scalar concentration gradient are compared with an analytical closure model which provides evolution equations for the mean passive scalar flux and variance. Triple correlations of fluctuations appearing in these equations are described in terms of relaxation terms proportional to the quadratic correlations. Three methods are used to extract the relaxation timescales τ_i from DNSs. Firstly, we insert the closure ansatz into our equations, assume stationarity and solve for τ_i . Secondly, we use only the closure ansatz itself and obtain τ_i from the ratio of quadratic and triple correlations. Thirdly, we remove the imposed passive scalar gradient and fit an exponential law to the decaying solution. We vary the Reynolds (Re) and Péclet numbers (while fixing their ratio at unity) and the degree of scale separation and find for large Re a fair correspondence between the different methods. The ratio of the turbulent relaxation time of the passive scalar flux to the turnover time of the turbulent eddies is of the order of 3, which is in remarkable agreement with earlier work. Finally, we make an effort to extract the relaxation timescales relevant for the viscous and diffusive effects. We find two regimes that are valid for small and large Re , respectively, but the dependence of the parameters on scale separation suggests that they are not universal.

PACS numbers: 47.27.E-, 47.27.tb, 47.40.-x

(Some figures may appear in colour only in the online journal)

1. Introduction

Fluid flows in astrophysical bodies are most often highly turbulent. Direct numerical simulations (DNSs) of such high-Reynolds-number flows are currently impossible. Consequently, greatly enhanced diffusivities or modified diffusion operators are often applied in simulations [6]. Such models are still challenging in terms of the required computational resources, so wide-ranging parameter studies cannot be conducted.

An alternative approach is to separate the large- and small scale quantities and derive equations for the former in which correlations of small scale quantities are

parameterized. This is usually referred to as mean-field theory, see e.g. [16, 20, 24, 25]. Various schemes have been introduced to close the equations for the correlations of small scale quantities. In astrophysics, the second-order correlation approximation (SOCA) and the (minimal) τ approximation (MTA; see, e.g., [1, 2]) are widely used where the latter invokes a relaxation term to approximate the higher-order correlations. The corresponding relaxation time has been determined numerically, e.g., for the α effect in mean-field electrodynamics [8, 9]. Another application of the MTA idea has been introduced in [21] in the context of mean-field hydrodynamics. In this ‘Ogilvie approach’ several non-dimensional coefficients are invoked to describe

physically motivated parameterizations of the higher-order correlations in the form of relaxation and isotropization terms. This model has been applied to different physical setups to calibrate the coefficients [12, 13, 17, 19].

The validity of the various approximations can, in principle, be tested by comparing with DNSs in the same parameter regime. In practice, this is often not easy because of the limited parameter range accessible by such simulations. The starting point for corresponding studies has been isotropically forced homogeneous turbulence under the influence of rotation [15] and/or shear [27]. A first systematic attempt to validate the τ approach in the passive scalar case was made in [5]. There, an ansatz for the mean flux of the scalar containing the relaxation time as the only unknown parameter was studied. Numerical experiments of three different types were performed to determine this relaxation time and yielded reasonably coinciding results, which were also consistent with analytic estimates.

In a recent work [26], the model parameters related to relaxation and isotropization that appear in the Ogilvie approach have been studied.

With the present study we turn again to the passive scalar case pursuing a threefold goal. We include a closure model for the mean concentration variance in the analysis in order to obtain hints on the viability of the analogous Ogilvie approach for the mean temperature variance. Further, we extend the parameter space to higher-scale separations, as well as both higher and lower Reynolds numbers compared to [5], and study the dependence of the closure parameters on these characteristics. This allows us to obtain insight into the level of universality of the ansatz parameters. In doing so, we employ three independent methods for determining the parameters, one of which has already been used in [5]. By making a comparison of their results, conclusions will be drawn about the completeness of the closure ansatzes.

The plan of the paper is as follows. In section 2, we provide its theoretical foundation by deriving the mean-field models on the basis of MTA, clarify their relationship to traditional mean-field results and establish the three methods we employ for testing the ansatzes. Section 3 describes our numerical setup and section 4 presents the results with a focus on comparisons between the outcomes of the different methods. In section 5, some comments and extensions are given and we draw our conclusions in section 6.

2. Mean-field modelling

2.1. Ideal case

Let us consider the transport of a passive scalar under the influence of a turbulent fluid motion. For simplicity we assume a homogeneous, incompressible fluid and neglect at first diffusion and viscous dissipation. Then the governing equations for the concentration of the passive scalar, C , and the fluid velocity \mathbf{U} read

$$\frac{\partial C}{\partial t} = -\nabla \cdot (\mathbf{U}C) = -\mathbf{U} \cdot \nabla C, \quad (1)$$

$$\frac{\partial \mathbf{U}}{\partial t} = -\mathbf{U} \cdot \nabla \mathbf{U} - \frac{1}{\rho} \nabla P + \mathbf{F}, \quad \nabla \cdot \mathbf{U} = 0, \quad (2)$$

where P is the pressure, ρ is the constant density and \mathbf{F} is a forcing function with $\nabla \cdot \mathbf{F} = 0$ (and with the unit ‘force per mass’). Upon introduction of a Reynolds averaging procedure, indicated by an overbar, C and \mathbf{U} are decomposed into mean and fluctuating parts, $C = \overline{C} + c$, $\mathbf{U} = \overline{\mathbf{U}} + \mathbf{u}$. The fluctuating fields, represented by lower-case letters, are then governed by

$$\frac{\partial c}{\partial t} = -\mathbf{u} \cdot \nabla \overline{C} - \overline{\mathbf{U}} \cdot \nabla c - (\mathbf{u} \cdot \nabla c)', \quad (3)$$

$$\frac{\partial \mathbf{u}}{\partial t} = -\mathbf{u} \cdot \nabla \overline{\mathbf{U}} - \overline{\mathbf{U}} \cdot \nabla \mathbf{u} - (\mathbf{u} \cdot \nabla \mathbf{u})' - \frac{1}{\rho} \nabla p + \mathbf{f}, \quad (4)$$

where the prime indicates extraction of the fluctuating part, e.g. $(\mathbf{u}c)' = \mathbf{u}c - \overline{\mathbf{u}c}$. Simplifying further, we stipulate the absence of a mean velocity $\overline{\mathbf{U}}$ and assume that the forcing has no mean part, i.e. $\mathbf{F} = \mathbf{f}$. In the present case, the goal of mean-field modelling consists in deriving a closed equation for the mean concentration \overline{C} . From (1) and (3), together with $\overline{\mathbf{U}} = \mathbf{0}$ we obtain directly

$$\frac{\partial \overline{C}}{\partial t} = -\nabla \cdot \overline{\mathcal{F}} \quad (5)$$

with the mean density of the passive scalar flux, $\overline{\mathcal{F}} = \overline{c\mathbf{u}}$. So the task of closing (5) reduces to representing $\overline{\mathcal{F}}$ by the mean concentration \overline{C} . In the standard mean-field approach, (3) is solved for a prescribed fluctuating velocity \mathbf{u} , usually under some simplifying assumptions which inevitably limit the applicability of the obtained results. The solution is employed to express $\overline{\mathcal{F}}$ in terms of \overline{C} . Alternatively, one can abstain from deriving such an explicit solution for the fluctuating concentration c and instead strive to establish an *evolution equation* for $\overline{\mathcal{F}}$ which of course again has to be closed in the sense that the only variables occurring are the mean quantities \overline{C} and $\overline{\mathcal{F}}$ themselves. Such an equation is obtained by multiplying (3) with \mathbf{u} and (4) with c , summing up and averaging, arriving at

$$\frac{\partial \overline{\mathcal{F}}}{\partial t} = -\overline{\mathbf{u}\nabla \cdot (\mathbf{u}\overline{C})} - \overline{\mathbf{u}\nabla \cdot (\mathbf{u}c)} - \overline{c\mathbf{u} \cdot \nabla \mathbf{u}} - \frac{1}{\rho} \overline{c\nabla p + c\mathbf{f}}. \quad (6)$$

By virtue of the incompressibility of the fluid, the fluctuating pressure p can be expressed by the velocity fluctuations:

$$\nabla^2 p = -\rho \left(\frac{\partial u_i}{\partial x_j} \frac{\partial u_j}{\partial x_i} \right)' \quad (7)$$

which, for an infinitely extended medium and vanishing p at infinity, is readily solved by

$$p = \frac{\rho}{4\pi} \int \frac{(\partial u_i / \partial x_j \partial u_j / \partial x_i)'(\mathbf{x}')}{|\mathbf{x} - \mathbf{x}'|} d^3x'. \quad (8)$$

Now we can conclude that the second, third and fourth terms on the rhs of (6) are quadratic in \mathbf{u} and linear in c , hence they represent third-order correlations. Following [13], we introduce here the *closure assumption* (τ ansatz):

$$-\overline{\mathbf{u}\nabla \cdot (\mathbf{u}c)} - \overline{c\mathbf{u} \cdot \nabla \mathbf{u}} - \frac{1}{\rho} \overline{c\nabla p} = -\frac{\overline{\mathcal{F}}}{\tau} \quad (9)$$

with a *relaxation time* τ_6 . Here the choice of the subscript 6 (and later 7) follows a convention introduced in [13]. Upon further neglect of the correlation $\overline{c\mathbf{f}}$, we arrive at

$$\frac{\partial \overline{\mathcal{F}}_i}{\partial t} = -\overline{u_i u_j} \frac{\partial \overline{\mathcal{C}}}{\partial x_j} - \frac{\overline{\mathcal{F}}_i}{\tau_6} = -\overline{\mathcal{R}}_{ij} \frac{\partial \overline{\mathcal{C}}}{\partial x_j} - \frac{\overline{\mathcal{F}}_i}{\tau_6}, \quad (10)$$

which governs the evolution of $\overline{\mathcal{F}}$. Here, $\overline{\mathcal{R}}_{ij} = \overline{u_i u_j}$ stands for the Reynolds stress tensor. Since a *passive* scalar would not act back onto the velocity, $\overline{\mathcal{R}}_{ij}$ can here be considered given and the closure is complete. Note that, in the presence of rotation or shear, (4) contributes further quadratic correlations to (6); see, e.g., [15, 18, 27].

Quite analogously, in [2] an evolution equation for the quantity $\nabla \cdot \overline{\mathcal{F}}$ instead of $\overline{\mathcal{F}}$ was derived where the triple correlation terms subsumed into the τ ansatz consequently contained one further spatial derivative in comparison to the terms in (9). Equation (10) is furthermore similar to the penultimate row of (53) in [13] when replacing the mean temperature perturbation $\overline{\Theta}$ by $\overline{\mathcal{C}}$ and neglecting the buoyancy term. Note that for small τ_6 , that is, fast relaxation, $\overline{\mathcal{F}}_i$ will follow the inhomogeneity in (10) almost instantaneously, hence

$$\overline{\mathcal{F}}_i \approx -\tau_6 \overline{\mathcal{R}}_{ij} \frac{\partial \overline{\mathcal{C}}}{\partial x_j}, \quad (11)$$

and we may interpret $\tau_6 \overline{\mathcal{R}}_{ij}$ as a *turbulent diffusivity tensor*. We return to a discussion of its relationship to traditional mean-field results in section 2.4.

To facilitate further comparisons to [4, 13], where an additional evolution equation for the mean temperature perturbation variance $\overline{\Theta^2}$ is derived, we give here an analogous equation for $\overline{c^2} = \overline{\mathcal{Q}}$, although it is in our case not necessary for completing the closure:

$$\frac{\partial \overline{\mathcal{Q}}}{\partial t} = -2\overline{c\mathbf{u}} \cdot \nabla \overline{\mathcal{C}} - 2\overline{c\mathbf{u}} \cdot \nabla c. \quad (12)$$

We note in passing that the quantity $\overline{\mathcal{Q}}$ becomes important in chemically reacting flows [4]. Setting

$$-2\overline{c\mathbf{u}} \cdot \nabla c = -\overline{\mathcal{Q}}/\tau_7 \quad (13)$$

with another relaxation time τ_7 , the closed equation reads

$$\frac{\partial \overline{\mathcal{Q}}}{\partial t} = -2\overline{\mathcal{F}} \cdot \nabla \overline{\mathcal{C}} - \frac{\overline{\mathcal{Q}}}{\tau_7} \quad (14)$$

and we have full analogy to the last row of (53) in [13].

Until now we have not constrained the properties of the turbulence; in particular, we have not required its isotropy or homogeneity. For example, inhomogeneous turbulence could be thought of as giving rise to position-dependent relaxation times $\tau_{6,7}$. However, we have to recall that the τ ansatz (9) implies that the only direction available to construct a vector is the one of $\overline{\mathcal{F}}$. Hence from a strict point of view, this ansatz is only consistent with an isotropic or *uni-axial* \mathbf{u} turbulence⁴ the preferred direction of which coincides with that of $\overline{\mathcal{F}}$. Consequently, as inhomogeneity always implies

anisotropy, turbulent properties of \mathbf{u} must not change along any other direction. The same restrictions should of course hold for the concentration fluctuations c ; yet this is in general in conflict with the presence of a second preferred direction in the correlation properties of this turbulence, namely the direction of $\nabla \overline{\mathcal{C}}$. Hence, (9) can be strictly justified only under the very specific circumstance that $\overline{\mathcal{F}}$ and $\nabla \overline{\mathcal{C}}$ are parallel (or anti-parallel) and their direction coincides with a possible preferred direction of \mathbf{u} .

For that reason and for the sake of simplicity, we specify now the mean as horizontal average, i.e. as average over all x and y . Consequently, all mean quantities depend on z only and only the z component of $\overline{\mathcal{F}}$ is relevant. If we further restrict \mathbf{u} to have at best a z anisotropy, then there is indeed only a single preferred direction, namely that of $\overline{\mathcal{F}}$ and the ansatz (9) is legitimate. The system of mean field equations then simplifies to

$$\begin{aligned} \frac{\partial \overline{\mathcal{C}}}{\partial t} &= -\frac{\partial \overline{\mathcal{F}}_z}{\partial z}, & \frac{\partial \overline{\mathcal{F}}_z}{\partial t} &= -\overline{\mathcal{R}}_{zz} \frac{\partial \overline{\mathcal{C}}}{\partial z} - \frac{\overline{\mathcal{F}}_z}{\tau_6}, \\ \frac{\partial \overline{\mathcal{Q}}}{\partial t} &= -2\overline{\mathcal{F}}_z \frac{\partial \overline{\mathcal{C}}}{\partial z} - \frac{\overline{\mathcal{Q}}}{\tau_7}, \end{aligned} \quad (15)$$

where $\overline{\mathcal{R}}_{zz}$, τ_6 and τ_7 can in principle still depend on z and t . However, with these quantities taken to be constant, that is, assuming homogeneous and statistically stationary fluctuations \mathbf{u} , the combination of the first two equations results in a 1D damped (for $\tau_6 > 0$) wave equation for $\overline{\mathcal{C}}$

$$\frac{\partial^2 \overline{\mathcal{C}}}{\partial t^2} + \frac{1}{\tau_6} \frac{\partial \overline{\mathcal{C}}}{\partial t} = \overline{\mathcal{R}}_{zz} \frac{\partial^2 \overline{\mathcal{C}}}{\partial z^2}, \quad (16)$$

guaranteeing a finite propagation speed of perturbations of $\overline{\mathcal{C}}$ [5]. A corresponding wave equation for the propagation of temperature perturbations was first proposed in [11].

Adopting a uniform gradient of $\overline{\mathcal{C}}$, $\nabla \overline{\mathcal{C}} = (0, 0, G)$, $G = \text{const}$, a stationary regime of (15) should be given by

$$\overline{\mathcal{F}}_z = \text{const} = -\tau_6 \overline{\mathcal{R}}_{zz} G, \quad \overline{\mathcal{Q}} = -2\tau_7 \overline{\mathcal{F}}_z G = 2\tau_6 \tau_7 \overline{\mathcal{R}}_{zz} G^2. \quad (17)$$

Let us now assume that in a DNS, equations (1) and (2) with an appropriately defined forcing \mathbf{f} and an imposed uniform $\nabla \overline{\mathcal{C}}$ are integrated in time until a statistically stationary regime is established. Extracting now all mean quantities occurring in (17) from the numerical solution and applying these relations, it is possible to determine the crucial relaxation times $\tau_{6,7}$ from such runs (method M1). On the other hand, $\tau_{6,7}$ should of course also obey their defining relations (9) and (13). The third-order correlations $\overline{\mathbf{u} \nabla \cdot (c\mathbf{u})}$, $\overline{c\mathbf{u} \cdot \nabla \mathbf{u}}$, $\overline{c \nabla p}$ and $\overline{c\mathbf{u} \cdot \nabla c}$ are again accessible in the DNS results and open up an independent path for determining the relaxation times (method M2). At the same time, it can also be checked to what extent the neglect of $\overline{c\mathbf{f}}$ is justified.

Another approach to extracting $\tau_{6,7}$ is available from decay experiments, for which, after having reached a stationary state in the DNS, the imposed gradient of $\overline{\mathcal{C}}$ is switched off. Then, according to (10) and (14), $\overline{\mathcal{F}}$ and $\overline{\mathcal{Q}}$ should decay uniformly in space and exponentially in time with the increment τ_6^{-1} and τ_7^{-1} , respectively, which can be identified with the decay rates measured in the DNS (method M3).

⁴ A velocity field whose turbulent properties, expressed, e.g., by its correlation tensor $\overline{u_i(\mathbf{x} + \boldsymbol{\xi}, t + \tau) u_j(\mathbf{x}, t)}$, are invariant under rotations about this axis, its 'preferred direction', but not under rotations about other axes.

The goal of this paper is to systematically test the validity of the presented closure assumptions for a range of Reynolds and Péclet numbers as well as different levels of separation between the spatial scales of mean and fluctuating fields. From this we expect hints with respect to the validity of the model of Garaud *et al* [13] for turbulent convection.

2.2. Non-ideal effects

Admitting now diffusion and viscous dissipation, we have to add the terms $\kappa \nabla^2 C$ with the diffusivity κ on the rhs of (1) and $\nu \nabla^2 \mathcal{U}$ with the kinematic viscosity ν on the rhs of (2). Consequently, in the evolution equation (6) for $\overline{\mathcal{F}}$, the additional terms $\overline{\nu c \nabla^2 \mathbf{u}}$ and $\overline{\kappa \mathbf{u} \nabla^2 c}$ occur on its rhs. Rewriting their sum as

$$\nu \nabla^2 \overline{\mathcal{F}_i} - 2\nu \overline{\nabla \cdot c \nabla \cdot \mathbf{u}_i} + (\kappa - \nu) \overline{u_i \nabla^2 c} \quad (18)$$

or more symmetric, as done in [13], as

$$\frac{\nu + \kappa}{2} \nabla^2 \overline{\mathcal{F}_i} - (\nu + \kappa) \overline{\nabla \cdot c \nabla \cdot \mathbf{u}_i} + \frac{\nu - \kappa}{2} \overline{c \nabla^2 u_i - u_i \nabla^2 c} \quad (19)$$

does nevertheless not allow a representation entirely by the mean flux. Even in the (very particular) case $\kappa = \nu$ the second terms of (18) and (19) remain. As a skyhook, the second and third terms in (19) are replaced by the τ -ansatz-like expression, $-\overline{\mathcal{F}}/\tau_{\nu\kappa}$, although they contain second-order rather than third-order correlations. Analogously, on the rhs of (12), diffusion requires a term

$$2\kappa \overline{c \nabla^2 c} = \kappa \nabla^2 \overline{Q} - 2\kappa \overline{(\nabla c)^2} \quad (20)$$

and the second term is replaced by $-\overline{Q}/\tau_{\kappa\kappa}$. Note that diffusion of $\overline{\mathcal{F}}$ and \overline{Q} modelled by the Laplacian terms in (18) and (20) is determined by the *molecular* (or microscopic) diffusivities.

In astrophysical applications the deviation from ideal conditions is usually small, and quantities expressing this smallness are given by the Reynolds and Péclet numbers, Re and Pe , which reflect the strength of advection relative to diffusion:

$$Re = u_{\text{rms}} \ell / \nu, \quad Pe = u_{\text{rms}} \ell / \kappa, \quad (21)$$

where ℓ is a characteristic length scale of the turbulence. We will further make use of the Schmidt number $Sc = \nu / \kappa = Pe / Re$.

2.3. Scaling of the relaxation times

For the relaxation times $\tau_{6,7,\nu\kappa,\kappa\kappa}$ some reasonable scaling assumptions are in order and we follow essentially the choices of [13]: $\tau_{6,7}$, belonging to third-order correlation terms, are expressed as $(C_{6,7} u_{\text{rms}} k_1)^{-1}$, and $\tau_{\nu\kappa,\kappa\kappa}$, belonging to diffusive second-order correlation terms, are written as

$$(C_{\nu\kappa} (\nu + \kappa) k_1^2 / 2)^{-1} \quad \text{and} \quad (C_{\kappa\kappa} \kappa k_1^2)^{-1}, \quad (22)$$

respectively. Here $k_1 = 2\pi/L$ is the smallest wavenumber consistent with the size of the system, L . The first of these

expressions seems to be appropriate only for $|\nu - \kappa| \ll \nu + \kappa$, hence in general the scaling ansatz should read instead

$$\left(\left(C_{\nu\kappa} \frac{\nu + \kappa}{2} + C_{\nu-\kappa} (\nu - \kappa) \right) k_1^2 \right)^{-1}, \quad (23)$$

The crucial question now is the following: are the constants $C_{6,7,\nu\kappa,\kappa\kappa}$ (or $C_{6,7,\nu+\kappa,\nu-\kappa,\kappa\kappa}$) universal, at least for a given type of turbulence, and in particular, are they independent of the dimensionless numbers of the problem, i.e. Re and Pe , and the degree of scale separation? A preliminary answer to this question was given in [5], where the timescales were found to show a slightly increasing trend with increasing scale separation (see figure 4 therein).

Methods M1 and M3 for determining the relaxation times described in section 2.1 have now to be modified in the following way: in (17) we have to replace τ_6 by $\tau_6 \tau_{\nu\kappa} / (\tau_6 + \tau_{\nu\kappa}) \equiv \tau_{6\nu\kappa}$ and τ_7 by $\tau_7 \tau_{\kappa\kappa} / (\tau_7 + \tau_{\kappa\kappa}) \equiv \tau_{7\kappa\kappa}$. Both methods then deliver only these aggregates and we have to employ the different scalings of the relaxation times to figure out the individual constants C_* . In contrast, method M2 merely has to be extended to include the additional second-order correlations showing up in (19) and (20), that is, to use instead of (9) and (13)

$$\begin{aligned} \frac{\overline{\mathcal{F}_z}}{\tau_{6\nu\kappa}} &= \overline{u_z \nabla \cdot (\mathbf{u}c)} + \overline{c \mathbf{u} \cdot \nabla u_z} + \frac{1}{\rho} \overline{c \nabla_z p} \\ &+ (\nu + \kappa) \overline{\nabla c \cdot \nabla u_z} - \frac{\nu - \kappa}{2} \overline{(c \nabla^2 u_z - u_z \nabla^2 c)}, \quad (24) \end{aligned}$$

$$\frac{\overline{Q}}{\tau_{7\kappa\kappa}} = 2 \left(\overline{c \mathbf{u} \cdot \nabla c} + \kappa \overline{(\nabla c)^2} \right). \quad (25)$$

2.4. Comparison with traditional results

A standard mean-field approach to (1), employing SOCA, that is, neglecting $(\mathbf{u} \cdot \nabla c)'$ in (3), yields for $\overline{\mathbf{U}} = \mathbf{0}$ straightforwardly (arguments \mathbf{x} dropped)

$$\overline{\mathcal{F}_i}(t) = - \int_0^\infty \overline{u_i(t) u_j(t - \tau)} \frac{\partial \overline{C}}{\partial x_j}(t - \tau) d\tau \quad (26)$$

from which, under the assumption of sufficient *temporal scale separation*,

$$\overline{\mathcal{F}_i}(t) = - \int_0^\infty \overline{u_i(t) u_j(t - \tau)} d\tau \frac{\partial \overline{C}}{\partial x_j}(t) = -\kappa_{ij} \frac{\partial \overline{C}}{\partial x_j}(t) \quad (27)$$

can be derived. $\kappa_{ij} = \int_0^\infty \overline{u_i(t) u_j(t - \tau)} d\tau = \tau_c \overline{u_i(t) u_j(t)}$ can be readily identified as turbulent diffusivity tensor with the correlation time τ_c just defined by the last identity. This clearly resembles the result (11) with τ_6 being identified with the correlation time τ_c , all the more so because for the validity of both (27) and (11) the relevant time parameter has, in a sense, to be small.

Relaxing the assumption of sufficient temporal scale separation, that is, retaining (26), we observe the presence of the so-called *memory effect* [14], that is, the influence of $\partial \overline{C} / \partial x_j$ at earlier times $t - \tau$ on the mean flux at time t by virtue of a convolution. Performing a Fourier transform

with respect to time, this convolution turns into a simple multiplication and we can write

$$\hat{\mathcal{F}}_i(\omega) = -\hat{\kappa}_{ij}(\omega) \hat{G}(\omega) \quad (28)$$

with a frequency-dependent turbulent diffusivity tensor $\hat{\kappa}_{ij}$. This quantity is directly accessible to the test-field method with time-dependent test fields as described in [14]. Based on numerical simulations and without resorting to SOCA, it has been found that for statistically stationary homogeneous isotropic turbulence a satisfactory approximation is accomplished already by

$$\hat{\kappa}_{ij}(\omega) = \delta_{ij} \frac{\kappa_0}{1 - i\omega\tau_\kappa}, \quad (29)$$

where κ_0 is the turbulent diffusivity for stationary fields and τ_κ is roughly independent of ω . A slightly better fit is provided by

$$\hat{\kappa}_{ij}(\omega) = \delta_{ij} (1 + K) \kappa_0 \frac{1 - i\omega\tau_\kappa}{(1 - i\omega\tau_\kappa)^2 + K} \quad (30)$$

with a constant K . Turning back to the physical space, the first approximation (29) is equivalent to

$$\overline{\mathcal{F}} + \tau_\kappa \frac{\partial \overline{\mathcal{F}}}{\partial t} = -\kappa_0 \nabla \overline{C} \quad (31)$$

or

$$\frac{\partial \overline{\mathcal{F}}}{\partial t} = -\frac{\kappa_0}{\tau_\kappa} \nabla \overline{C} - \frac{\overline{\mathcal{F}}}{\tau_\kappa}. \quad (32)$$

Again, there is striking similarity to (10). Thus, by comparing τ_6 to numerical results for τ_κ , a further independent way of checking (9) is provided. The second fit (30) yields [14]

$$(1 + K) \overline{\mathcal{F}} + 2\tau_\kappa \frac{\partial \overline{\mathcal{F}}}{\partial t} + \tau_\kappa^2 \frac{\partial^2 \overline{\mathcal{F}}}{\partial t^2} = -(1 + K) \kappa_0 \nabla \left(\overline{C} + \tau_\kappa \frac{\partial \overline{C}}{\partial t} \right) \quad (33)$$

indicating the potential importance of higher temporal derivatives of $\overline{\mathcal{F}}$ and mixed temporal/spatial derivatives of \overline{C} . Note that (32) and (33) are only valid for perfect scale separation in space.

The case of perfect temporal but imperfect spatial scale separation was studied in [10]. Complementary to (28), now a Fourier transform with respect to space has to be performed and we are faced with a diffusivity tensor depending on the wavevector \mathbf{k} . In the isotropic case with horizontal average a reasonable fit is [10]

$$\hat{\kappa}_{ij}(k_z) = \delta_{ij} \frac{\kappa_0}{1 + \ell^2 k_z^2}, \quad (34)$$

which gives rise to

$$\overline{\mathcal{F}} - \kappa_{\mathcal{F}} \tau_0 \nabla^2 \overline{\mathcal{F}} = -\kappa_0 \nabla \overline{C} \quad (35)$$

in physical space, resembling (10) with (18) or (19) for the stationary regime. Here, $\kappa_{\mathcal{F}}$ is an additional diffusivity of $\overline{\mathcal{F}}$, τ_0 is the dynamical time and $\kappa_{\mathcal{F}} \tau_0 = \ell^2$. $\kappa_{\mathcal{F}}$ has been found to be of the order of the SOCA estimate of the turbulent diffusivity in the low-diffusivity limit, $\kappa_t = \tau_c u_{\text{rms}}^2 / 3$. Clearly, this value can be very different from the molecular diffusivity.

For the general case of imperfect scale separation with respect to both space and time, see [23], albeit that work

deals with the mean electromotive force $\overline{\mathcal{E}}$ of MHD rather than with the mean flux of passive scalar transport. In that work, non-locality due to imperfect spatial scale separation shows up again in the form of a diffusion term $\eta_\varepsilon \nabla^2 \overline{\mathcal{E}}$ in the evolution equation for $\overline{\mathcal{E}}$ with a diffusivity η_ε of the order of the SOCA estimate of the turbulent diffusivity in the high-conductivity limit, $\eta_t = \tau_c u_{\text{rms}}^2 / 3$.

When comparing both results with the diffusion term for $\overline{\mathcal{F}}$ identified in (18) or (19) where only the microscopic diffusivities occur, we have to state that the τ approach deviates in this respect significantly from what we expect from the traditional one. To reconcile them, possible diffusion terms $\propto \nabla^2 \overline{\mathcal{F}}$ and $\propto \nabla^2 \overline{Q}$ had to be taken into account in the parameterizing ansatzes. This was not considered until now.

2.5. Significance of method comparisons

Let us finally discuss what is really ‘tested’ by comparisons of the results from the different methods M1–M3. For an incompressible fluid with the specific conditions of our model and under the assumption that no higher than the first-order temporal derivative of $\overline{\mathcal{F}}$ occurs, an ansatz analogous to (10),

$$\frac{\partial \overline{\mathcal{F}}_z}{\partial t} = -K_1 G - K_2 \overline{\mathcal{F}}_z, \quad (36)$$

is exhaustive, as

- (i) c and hence $\overline{\mathcal{F}}_z$ consist of two parts one of which is a linear and homogeneous functional of G and the other is independent of G and determined only up to an arbitrary scale factor. Of course these are consequences of the linearity of (3) (and do not depend on the neglect of $c\mathbf{f}$ in (6)).
- (ii) G and hence (for uniform initial conditions) $\overline{\mathcal{F}}_z$ are spatially constant, both in the statistically steady state and during the free decay of $\overline{\mathcal{F}}_z$. (That is why the diffusive term $\propto \nabla^2 \overline{\mathcal{F}}_z$ is absent in (36).)

Note, however, that $K_1 = \overline{\mathcal{R}}_{zz}$ as in (10) is an assumption (or a consequence of the assumption (24)) because a contribution proportional to $\nabla \overline{C}$ or $\partial \overline{\mathcal{F}}_z / \partial t$ could also be provided by the triple correlations, the diffusive terms, or by $c\mathbf{f}$.

Since the *passive* scalar C does not influence the turbulent velocity, the coefficients $K_{1,2}$ in (36) are completely determined by \mathbf{u} and hence true constants. Consequently, any comparison of the methods M1, M2 and M3 tests the influence of

- (i) deviations of the simulated velocity turbulence from homogeneity, isotropy and statistical stationarity and furthermore
- (ii) the weak compressibility of the fluid in our simulations.

Note that the first influence can, in principle, be made arbitrarily small by increasing scale separation and extending time ranges for averaging and likewise the second influence by increasing the sound speed c_s in the numerical model.

A comparison of M1 and M3 tests, in addition, the justification of

- (i) the neglect of higher temporal derivatives, and $\overline{\mathcal{F}}_z$, and
- (ii) the assumption $K_1 = \overline{\mathcal{R}}_{zz}$ that is employed in calculating $\tau_{6\nu\kappa} = 1/K_2$ from the steady state.

On the other hand, a comparison of M1 and M2 tests against the assumption $K_1 = \overline{\mathcal{R}}_{zz}$ and specifically to what extent the neglect of the correlation $c\mathbf{f}$ is legitimate.

With respect to $\overline{\mathcal{Q}}$, again assuming that only first-order temporal derivatives occur, the ansatz

$$\frac{\partial \overline{\mathcal{Q}}}{\partial t} = -K_3 \overline{\mathcal{F}}_z G - K_4 \overline{\mathcal{Q}} - K_5 \overline{\mathcal{F}}_z^2 - K_6 G^2 \quad (37)$$

is exhaustive for the same reasons listed after (36) when a uniform $\overline{\mathcal{Q}}$ is assumed. Consequently, a comparison of M1 and M3 tests here, apart from the general assumptions about the turbulence, the justification of

- (i) the neglect of higher-order temporal derivatives, and
- (ii) the assumption $K_5 = 0$ that enters the determination of $\tau_{7\kappa\kappa} = 1/K_4$ by M3, and also the assumption $K_3 - K_5 K_1/K_2 - K_6 K_2/K_1 = 2$ that enters M1. Note that $K_5 \neq 0$ would make the decay of $\overline{\mathcal{Q}}$, in general, non-exponential (a sum of two exponentials).

The second test of (ii) is also performed by the comparison of M1 and M2.

3. Numerical setup

In order to take advantage of the capabilities of the PENCIL CODE⁵, we solve instead of the incompressible system (1) and (2) the corresponding equations for a compressible but isothermal fluid

$$\frac{\partial \mathbf{U}}{\partial t} = -\mathbf{U} \cdot \nabla \mathbf{U} - \nabla H + \mathbf{f} + 2\nu (\nabla \cdot \mathbf{S}(\mathbf{U}) + \mathbf{S}(\mathbf{U}) \cdot \nabla H/c_s^2), \quad (38)$$

$$\frac{\partial H}{\partial t} = -\mathbf{U} \cdot \nabla H - c_s^2 \nabla \cdot \mathbf{U}, \quad (39)$$

$$\frac{\partial C}{\partial t} = -\nabla \cdot (C\mathbf{U}) + \kappa \nabla^2 C, \quad (40)$$

where we employ the pseudo-enthalpy $H = c_s^2 \ln \rho$ instead of the density; c_s is the constant speed of sound and $\mathbf{S}(\mathbf{U})$ is the trace-less rate-of-strain tensor $S_{ij} = (\partial U_i/\partial x_j + \partial U_j/\partial x_i)/2 - \delta_{ij} \nabla \cdot \mathbf{U}/3$. The interpretation of the results of such simulations in terms of the incompressible model, of course, requires keeping the Mach number u_{rms}/c_s small, typically < 0.1 . Then it is particularly justified to replace the correlation $c\nabla p/\rho$, included in the τ ansatz, by $c\nabla h$.

The equations are solved by equidistant sixth-order finite differences in space and an explicit third-order time stepping scheme with step size control for stability. The computational domain is a cube with dimension $(2\pi)^3$ and grid resolutions

ranging from 32^3 to 256^3 according to the requirements raised by the values of Re and Pe and the forcing wavenumber. Boundary conditions are periodic throughout. The fluctuating force \mathbf{f} is specified such that it generates an approximately homogeneous, isotropic and statistically stationary fluctuating velocity \mathbf{u} . Here, \mathbf{f} is a frozen-in linearly polarized (i.e. non-helical) random plane wave with a wavevector which is consistent with the periodic boundary conditions and whose modulus is close to a chosen average value k_f . The wave amplitude is kept fixed whereas the wavevector is randomly changing between time steps and hence \mathbf{f} is approximately δ -correlated in time. For further details, see [3].

4. Results

In general, the parameter space is spanned by the dimensionless numbers $s = k_f/k_1$ (degree of scale separation), Re and Pe , in whose definitions (21) we specify the characteristic length ℓ for simplicity by $1/k_f$. In the following, we will, however, restrict ourselves to $Re = Pe$, that is, $Sc = 1$ and leave the more general cases to future work. By this, we avoid, in particular, the complication with the scaling ansatz (23) that occurs for $\nu \neq \kappa$.

All proposed methods require the mean quantities $\nabla \overline{C}$, $\overline{\mathcal{Q}}$ and $\overline{\mathcal{F}}$ to be constant with respect to z . As the imposed gradient G is uniform, we expect that only the deviation of the turbulence from being perfectly homogeneous should perturb this constancy by causing small-amplitude wiggles of typically the scale of the forcing. However, it turns out that perturbations with considerable amplitudes occur regularly with dominating scales $2\pi/k_1$ or π/k_1 corresponding to the box size and its half. They can hardly be explained by an unstable solution of (16), say for a persistently negative τ_6 , because it would unlimitedly grow due to the lack of any back-reaction onto the flow. Instead we might think of an incoherent parametric excitation caused by occasional excursions of τ_6 into the negative similar to magnetic field generation by an incoherent shear-current effect, see [7]. However, the supposed excitation seems to act efficiently only if the imposed gradient G is present, whereas in the decay experiments all spectral constituents (in z) of the mean quantities decay, albeit with different rates. To enable the term $\overline{\mathcal{R}}_{zz} G$, occurring in the second of equations (15), to act on \overline{C} it is necessary to assume z -dependent fluctuations in $\overline{\mathcal{R}}_{zz}$. Although there is no reason why in these fluctuations low z wavenumbers are preferred (indeed the forcing wavenumber should be), the diffusion terms in the equations for $\overline{\mathcal{F}}$ and \overline{C} can provide for such a preference, at least in cases with low or moderate Re . With respect to $\overline{\mathcal{Q}}$ we note that excitation of z -dependent modes could also be accomplished by the terms $\propto \overline{\mathcal{F}}_z G$ and $\propto \overline{\mathcal{F}}_z^2$ in (37) provided that such modes are already present in $\overline{\mathcal{F}}_z$.

Summing up, strict obedience of the proposed methods' prerequisites requires the extension of our definition of the mean by a z average or, in other words, to define the mean as *volume average* over the entire box.

For methods M1 and M2, all averaged quantities were derived from the simulations by performing, in addition to the volume averaging, a temporal averaging over an interval in

⁵ Freely available at <http://pencil-code.googlecode.com/>

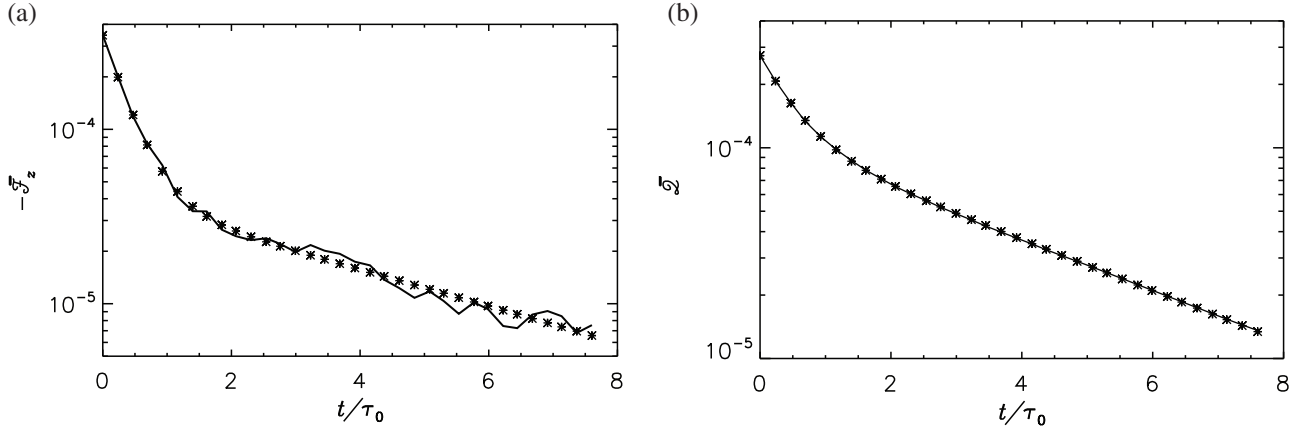


Figure 1. Decay of $\overline{\mathcal{F}}_z$ (left) and \overline{Q} (right) for $s = 3$, $Re = Pe \approx 1$. Solid line: DNS, symbols: fits with ansatz (41).

Table 1. Results from methods M1, M2 and M3 for different values of $s = k_f/k_1$, $\nu = \kappa$, $Sc = 1$. M3 results refer to the early decay times.

s	Re	M1		M2		M3	
		$\tau_{6\nu\kappa}$	$\tau_{7\kappa\kappa}$	$\tau_{6\nu\kappa}$	$\tau_{7\kappa\kappa}$	$\tau_{6\nu\kappa}$	$\tau_{7\kappa\kappa}$
1.5	0.26 ... 1148.55	0.13 ... 2.42	0.13 ... 4.28	0.13 ... 2.71	0.13 ... 4.26	0.13 ... 2.96	0.15 ... 5.21
3	0.09 ... 557.19	0.03 ... 2.64	0.03 ... 4.75	0.03 ... 2.70	0.03 ... 5.09	0.06 ... 2.81	0.05 ... 4.96
5	0.04 ... 331.17	0.01 ... 2.77	0.01 ... 5.21	0.01 ... 2.79	0.01 ... 6.06	0.03 ... 2.77	0.02 ... 5.67
8	0.02 ... 205.52	0.003 ... 2.86	0.005 ... 6.06	0.005 ... 2.88	0.005 ... 7.73	0.01 ... 2.85	0.01 ... 7.70
10	0.02 ... 163.24	0.002 ... 2.87	0.003 ... 6.56	0.003 ... 2.93	0.003 ... 8.93	0.006 ... 2.99	0.006 ... 4.50

which, in particular, \overline{Q} was found to be statistically stationary. We have observed that such a temporal average makes z averaging unnecessary for achieving z independence of the mean quantities. This is consistent with the supposition of a parametric mode excitation as it should act randomly and hence produce perturbations which are uncorrelated over long enough times. We have, however, always employed the volume average. Statistical errors were estimated by dividing the time interval into three equally long parts and calculating averages over each of them. These individual averages were compared to the average over the whole interval, and the largest deviation was taken for the error estimate.

In applying method M3 we were faced with the fact that only in rare cases the temporal behaviour of the mean quantities can be properly described by a single exponential. However, a fit to an ansatz with two exponentials, that is,

$$A_1 \exp(-t/\tau_1) + A_2 \exp(-t/\tau_2), \quad (41)$$

was in most cases suited for reproducing the simulation data with high fidelity, see figure 1. Almost always, the initial part of the decay process immediately after the switching off of the imposed gradient was governed by the higher decay rate, that is, the shorter of the two decay times $\tau_{1,2}$. Consequently, the exponential with the longer decay time took over later on. For this reason we denote the former as ‘early’ and the latter as ‘late’ decay time.

In the context of method M3 we have also made an attempt to estimate the coefficients of the Laplacians occurring in (19) and (20) by omitting the z average and subjecting $\overline{\mathcal{F}}_z(z)$ and $\overline{Q}(z)$ to a Fourier transform with respect to z . Then the coefficient of the Laplacian is $(\tau_n^{-1} - \tau_0^{-1})/n^2 k_1^2$ where τ_n , $n = 0, 1, \dots$, is the decay time of the n th z

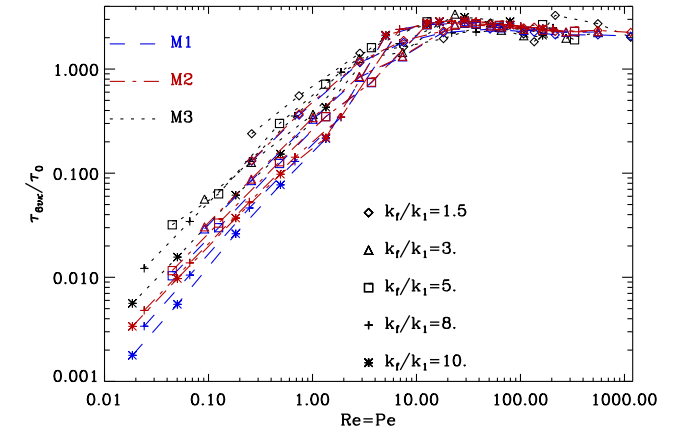


Figure 2. Relaxation time $\tau_{6\nu\kappa}$, normalized by the dynamical time $\tau_0 = (u_{rms} k_f)^{-1}$, as a function of $Re = Pe$ from methods M1–M3. Different symbols refer to different scale separations $s = k_f/k_1$ as indicated in the legend. M3 results refer to the early decay times.

harmonic of $\overline{\mathcal{F}}_z(z)$ and $\overline{Q}(z)$, respectively. Following the reasoning given with (19) and (20) this coefficient should for all $n > 0$ turn out to be $(\nu + \kappa)/2$ and κ , respectively. Unfortunately, corresponding results do not form a consistent picture.

We performed a number of simulations, and extracted $\tau_{6\nu\kappa}$ and $\tau_{7\kappa\kappa}$ using methods M1, M2 and M3. The results are summarized in table 1, where the simulations are grouped into different sets by the values used for the scale separation s . Within each set Re and Pe were varied by changing ν ($= \kappa$). The timescales $\tau_{6\nu\kappa}$ and $\tau_{7\kappa\kappa}$ listed in table 1 are also illustrated in figures 2 and 3, respectively. We see that all three methods give quite similar results, which grow with

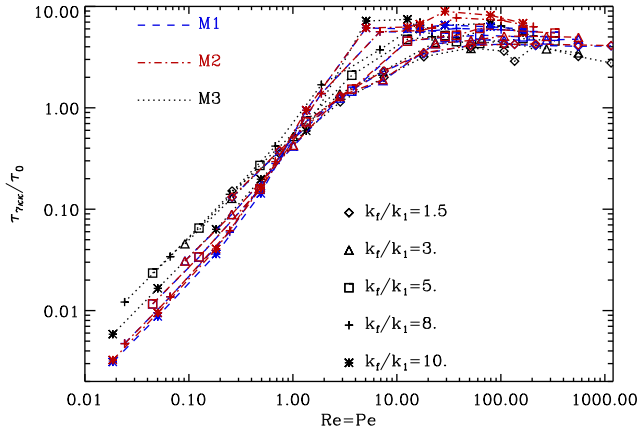


Figure 3. Relaxation time $\tau_{7\kappa\kappa}$ from methods M1–M3. For explanations see figure 2.

Re for $Re \lesssim 10$ and turn stationary for $Re \gtrsim 10$, where the timescales converge to

$$\tau_{6\nu\kappa}/\tau_0 \approx 2 \dots 3, \quad \text{and} \quad \tau_{7\kappa\kappa}/\tau_0 \approx 7 \dots 10. \quad (42)$$

There are some exceptions, however. When $s = 1.5$, all the methods M1–M3 yield $2 \lesssim \tau_{7\kappa\kappa}/\tau_0 \lesssim 5$, somewhat smaller values than obtained for larger scale separations. The results from method M3 tend to be somewhat larger than the results from the other methods for $Re < 10$, but for $Re > 10$ this difference mostly disappears.

4.1. Universality of the closure ansatz

As explained in section 2.3, methods M1 and M3 yield only the quantities $\tau_{6\nu\kappa}$ and $\tau_{7\kappa\kappa}$ from which the constants $C_{6,7,\nu\kappa,\kappa\kappa}$ can be extracted as follows. Recalling the scalings introduced in section 2.3 we have

$$\begin{aligned} \frac{1}{\tau_{6\nu\kappa}} &= C_6 u_{\text{rms}} k_1 + C_{\nu\kappa} (\nu + \kappa) \frac{k_1^2}{2}, \\ \frac{1}{\tau_{7\kappa\kappa}} &= C_7 u_{\text{rms}} k_1 + C_{\kappa\kappa} \kappa k_1^2. \end{aligned} \quad (43)$$

Multiplying by the viscous time $\tau_{\text{visc}} = (\nu k_1^2)^{-1}$ yields

$$\frac{1}{\tilde{\tau}_{6\nu\kappa}} = C_6 s Re + C_{\nu\kappa}, \quad \frac{1}{\tilde{\tau}_{7\kappa\kappa}} = C_7 s Pe + C_{\kappa\kappa}, \quad (44)$$

where a tilde indicates normalization by τ_{visc} . Hence, when considering $1/\tilde{\tau}_{6\nu\kappa}$ and $1/\tilde{\tau}_{7\kappa\kappa}$ as functions of Re (or Pe), the wanted parameters $C_{6,7,\nu\kappa,\kappa\kappa}$ should be obtainable by a linear regression analysis. Figure 4 shows both functions (44) from M1 for different values of s . A linear relation is clearly present both for large and small values of Re , but with very different fit parameters for the two ranges. Guided by these functional dependences we hence propose as an alternative for (44)

$$\frac{1}{\tilde{\tau}_{6\nu\kappa}} = C_6 s Re + C_{\nu\kappa} + \frac{1}{C'_6 s Re + C'_{\nu\kappa}} \equiv F(Re), \quad (45)$$

and analogously for $1/\tilde{\tau}_{7\kappa\kappa}$. This ansatz allows us to model linear dependences on Re for both small and large arguments,

but with different coefficients:

$$F(Re) \approx C_6 s Re + C_{\nu\kappa} \quad \text{for } Re \rightarrow \infty, \quad (46)$$

$$F(Re) \approx \left(C_6 - \frac{C'_6}{C'_{\nu\kappa}} \right) s Re + C_{\nu\kappa} + \frac{1}{C'_{\nu\kappa}} \quad \text{for } Re \rightarrow 0, \quad (47)$$

where the slopes may well be different in sign. The constants in (45) were determined by a standard fitting procedure and are given in table 2. For both relaxation times, the fit is surprisingly good with exceptions in $\tilde{\tau}_{7\kappa\kappa}$ for $s = 8, 10$ around $Re = 1$, see figure 4. The slopes for high Re , that is, C_6 and C_7 , show a possible saturation with growing scale separation s , but the other coefficients do not. Hence, the universality of the ansatz (45) with respect to scale separation is questionable for $s \leq 3$, as has already been found in [5].

4.2. Comparison of methods

Let us next compare the relaxation timescales obtained with the different methods in more detail.

4.2.1. Methods M1 and M3. Figure 5 shows the ratio of the values of $\tau_{6\nu\kappa}$ and $\tau_{7\kappa\kappa}$ determined by either of the two methods as functions of Re and s where the M3 values were identified with either the early or the late decay times. With some exceptions for $s = 1.5, 3, 5$ the early decay times from M3 differ from those from M1 only by up to $\pm 40\%$ where for $\tau_{6\nu\kappa}^{\text{early}}$ both signs appear roughly equally frequently while for $\tau_{7\kappa\kappa}^{\text{early}}$ the negative deviations clearly prevail. In the latter, the results show some erratic behavior for small Re and $s = 8, 10$ which might be caused by insufficient resolution. For the late values of both $\tau_{6\nu\kappa}$ and $\tau_{7\kappa\kappa}$, the results of method M3 deviate clearly from those of M1 with the exception of the lowest scale separation $s = 1.5$ and $s = 3$ (the latter for high Re only). In general, the deviations grow with falling Re and increasing s , but the latter tendency shows some saturation for the high values of s . Note that the determination of $\tau_{6\nu\kappa}^{\text{M3,late}}$ is generally subject to some uncertainties because of strong fluctuations showing up there.

Naturally, the question arises whether a relationship exists between the late decay times and the viscous = diffusive timescale for the scale of the domain, $\tau_{\text{diff}} = \tau_{\text{visc}} = 1/\kappa k_1^2 = 1/\nu k_1^2$, or the dynamical time τ_0 . Figure 6 shows $\tau_{6\nu\kappa}^{\text{M3,late}}$ and $\tau_{7\kappa\kappa}^{\text{M3,late}}$, normalized by τ_{visc} as functions of Re . As indicated by the red lines, these dependences can be represented rather well by functions $\propto 1/(1+Re)$ with amplitudes τ_{visc} and $\tau_{\text{visc}}/2$, respectively. This means, in other words, that for low Re the late decay times approach τ_{visc} and $\tau_{\text{visc}}/2$, respectively, whereas for high Re they approach $s^2\tau_0$ and $s^2\tau_0/2$, respectively. Remarkably, this seems to hold rather independently of the scale separation with some exceptions for $s = 1.5$ and 10 . This finding about the late values is consistent with the occurrence of the term $-K_5 \overline{\mathcal{F}}_z^2$ in (37): that term implies that the decay rate of $\overline{\mathcal{Q}}$ after the fading out of a possible constituent being a solution of the homogeneous part of (37) (with $G = 0$) is twice the decay rate of $\overline{\mathcal{F}}_z$. However, it remains unexplained why $\overline{\mathcal{F}}_z$ shows also a decay behaviour characterized by two exponentials as (36) gives no clue to that (but see the *note added in proof*).

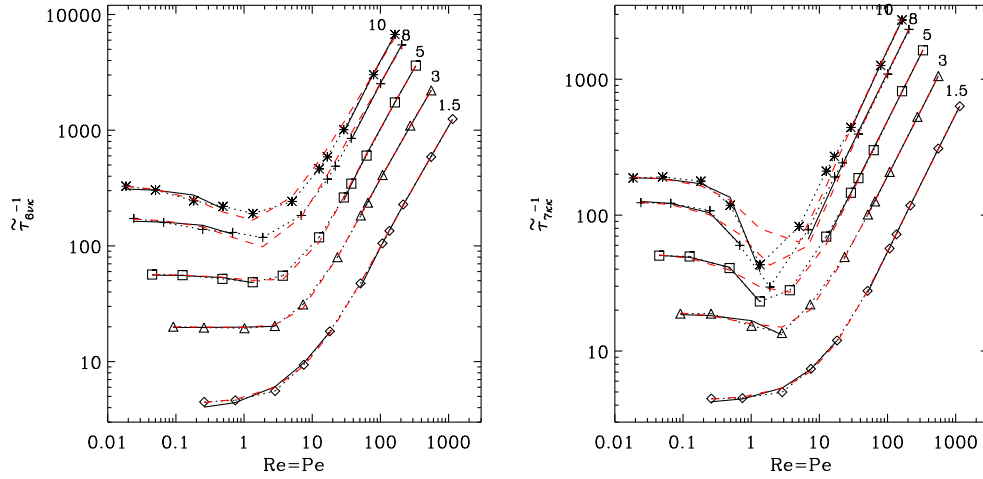


Figure 4. Relaxation times $\tilde{\tau}_{6\nu\kappa}$ (left) and $\tilde{\tau}_{7\kappa\kappa}$ (right), normalized to the viscous time τ_{visc} as functions of $Re = Pe$, for different values of the scale separation s , indicated at the curves. Dotted lines with symbols: the data from method M1; solid lines: linear fits according to (44), separately for low and high Re . Red dashed lines approximation by (45) with parameters $C_{6,7}$, $C'_{6,7}$, $C_{\nu\kappa,\kappa\kappa}$, $C'_{\nu\kappa,\kappa\kappa}$ from a best fit, see table 2.

Table 2. Fit parameters of the scaling (45) for the results of M1 shown in figure 4.

s	C_6	$C_{\nu\kappa}$	$10^4 C'_6$	$10^3 C'_{\nu\kappa}$	C_7	$C_{\kappa\kappa}$	$10^4 C'_7$	$10^2 C'_{\kappa\kappa}$
1.5	0.73	-17.78	7.33	45.33	0.37	-4.29	20.94	11.58
3	1.35	-30.71	6.17	19.71	0.63	2.38	94.64	5.80
5	2.22	-89.19	1.73	6.85	1.00	-8.22	23.28	1.65
8	3.22	-32.12	4.88	4.86	1.46	-45.80	6.12	0.58
10	3.83	52.11	9.16	3.48	1.75	-84.36	2.63	0.36

4.2.2. Methods M1 and M2. As can be seen in figure 7, for small scale separations $s = 1.5, 3, 5$ or for $Re \gtrsim 1$ the values of $\tau_{6\nu\kappa}$ from both methods coincide fairly well. Deviations lie within errors. For large $s = 8, 10$, however, we find the deviations growing with falling Re . We have to conclude that the neglect of $c\mathbf{f}$ and/or the deviation of K_1 from $\overline{\mathcal{R}}_{zz}$ (see section 2.5) has its strongest effects for low Re and high s . In contrast, the differences between the $\tau_{7\kappa\kappa}$ values from methods M1 and M2 are clearly smaller, reaching a significant magnitude (exceeding errors) only for small Re , $s = 10$ and for $20 \lesssim Re \lesssim 300$ and $s = 5, 8, 10$. A possible reason for this is again insufficient numerical resolution.

5. Comments and extensions

5.1. Alternative scaling

As an alternative to (43), one might consider

$$\frac{1}{\tau_{6\nu\kappa}} = C_6 u_{\text{rms}} k_f + C_{\nu\kappa} (\nu + \kappa) \frac{k_f^2}{2}, \quad \frac{1}{\tau_{7\kappa\kappa}} = C_7 u_{\text{rms}} k_f + C_{\kappa\kappa} \kappa k_f^2. \quad (48)$$

Then, by multiplying with the dynamic time $\tau_0 = (u_{\text{rms}} k_f)^{-1}$ we arrive at

$$\frac{1}{\tilde{\tau}_{6\nu\kappa}} = C_6 + \frac{C_{\nu\kappa}}{Re}, \quad \frac{1}{\tilde{\tau}_{7\kappa\kappa}} = C_7 + \frac{C_{\kappa\kappa}}{Pe}, \quad (49)$$

where the normalization is now with respect to τ_0 . Figure 8 shows the same results as figure 4, but now with the altered scaling. Again, a linear fit is viable on each curve, but

only separately for low and high Re . The corresponding fit parameters can be found in table 3. Unfortunately, an overall fit analogous to (45) does not work satisfactorily here. In striking contrast to figure 4, the lines for different s now lie very close together.

This is reflected by the fit parameters given in table 3: for small Re the values of $C_{\nu\kappa}$ and $C_{\kappa\kappa}$ show only less variance while for high Re this holds true for the values of C_6 and C_7 . So with the alternative scaling the model can be brought closer to universality with respect to s .

5.2. A τ approach for compressible hydrodynamics?

One could be tempted to treat the system (38)–(40) in the spirit of the τ approach in quite an analogous manner to what was shown in section 2.1. In the ideal case and with $\overline{\mathbf{U}} = \mathbf{0}$, $\overline{\mathbf{H}} = 0$, we have for the fluctuating fields

$$\frac{\partial \mathbf{u}}{\partial t} = -(\mathbf{u} \cdot \nabla \mathbf{u})' - \nabla h + \mathbf{f}, \quad (50)$$

$$\frac{\partial h}{\partial t} = -(\mathbf{u} \cdot \nabla h)' - c_s^2 \nabla \cdot \mathbf{u}, \quad (51)$$

and for the mean flux an analogue of (6), but with the term $-\overline{c\nabla p}/\rho$ replaced by $-\overline{c\nabla h}$. To close the system, an evolution equation for the quantity $\overline{c\nabla h}$ seems therefore to be indicated. From (3) (modified for compressibility) and (51)

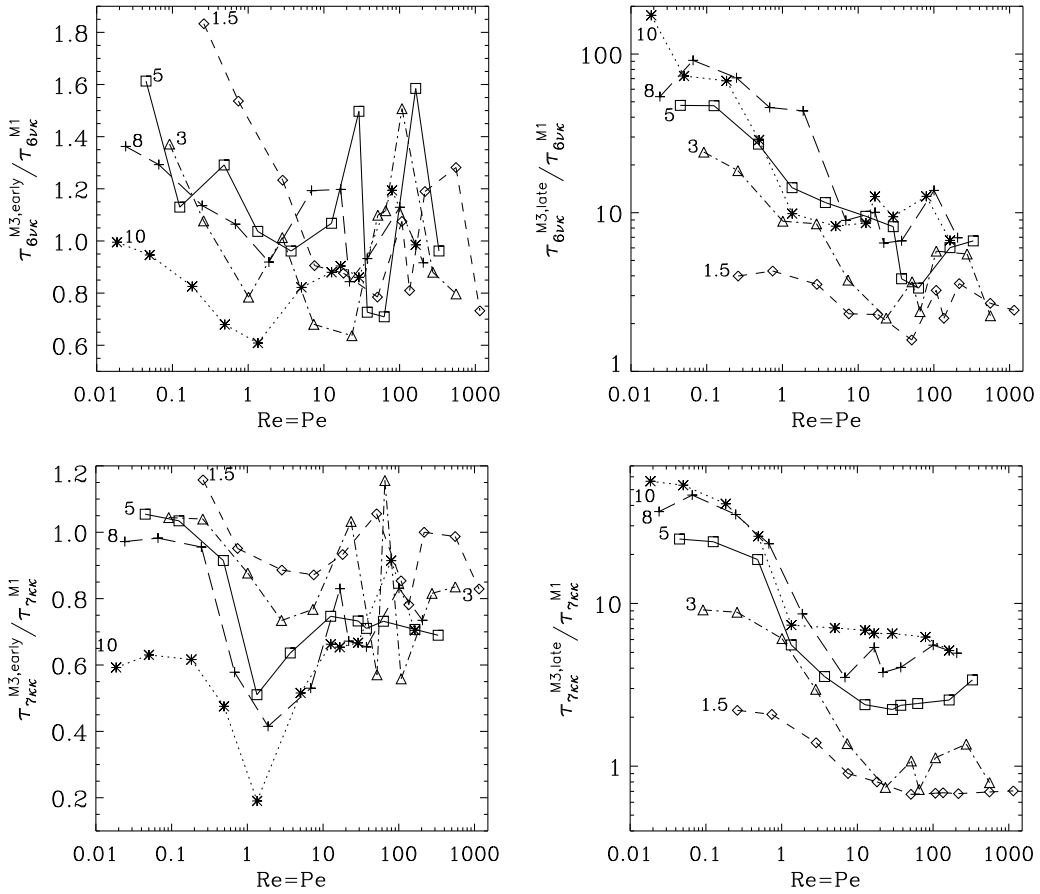


Figure 5. The ratio of the values of $\tau_{6\nu\kappa}$ (top) and $\tau_{7\kappa\kappa}$ (bottom) determined by methods M1 and M3. Left/right: early/late values. Labels: scale separation s .

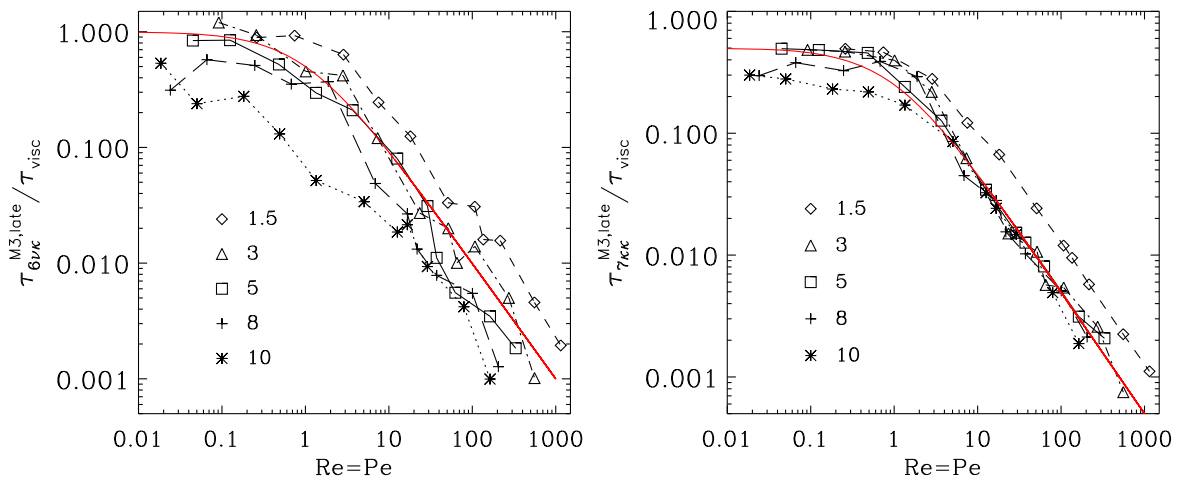


Figure 6. Broken lines, symbols: $\tau_{6\nu\kappa}^{M3,late}$ and $\tau_{7\kappa\kappa}^{M3,late}$ normalized by τ_{visc} from method M3. Red solid line: $\tau_{visc}/(1+Re)$ and $0.5\tau_{visc}/(1+Re)$, respectively. Values in the legend: scale separation s .

Table 3. Fit parameters of the alternative scaling (49) for the results shown in figure 8.

s	Small Re				Large Re			
	C_6	$C_{\nu\kappa}$	C_7	$C_{\kappa\kappa}$	C_6	$C_{\nu\kappa}$	C_7	$C_{\kappa\kappa}$
1.5	0.23	1.93	0.14	1.94	0.48	-3.64	0.24	-0.30
3	-0.065	2.23	-0.26	2.13	0.44	-1.62	0.21	0.29
5	-0.34	2.28	-0.77	2.05	0.44	-2.45	0.19	0.31
8	-1.63	2.72	-1.19	1.96	0.40	-1.07	0.17	0.05
10	-3.19	3.32	-0.84	1.90	0.39	-0.53	0.17	-0.46

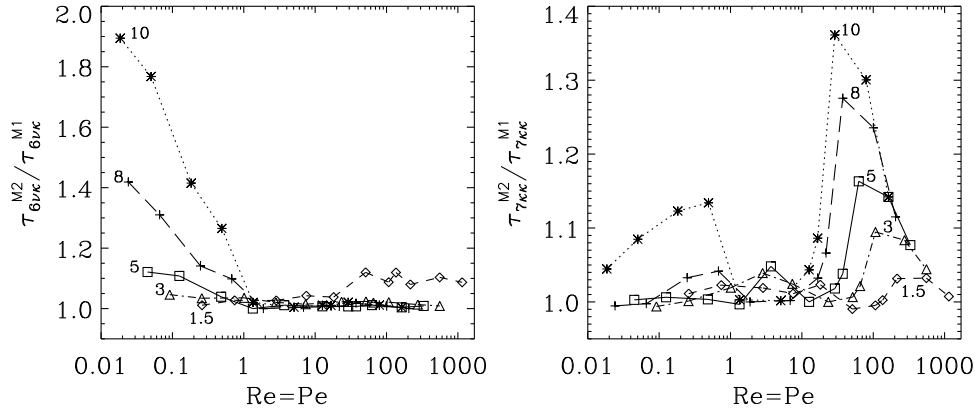


Figure 7. The ratio of the values of $\tau_{6v\kappa}$ (left) and $\tau_{7\kappa\kappa}$ (right) determined by methods M1 and M2. Labels; scale separation s . For symbol legend, see figure 6.

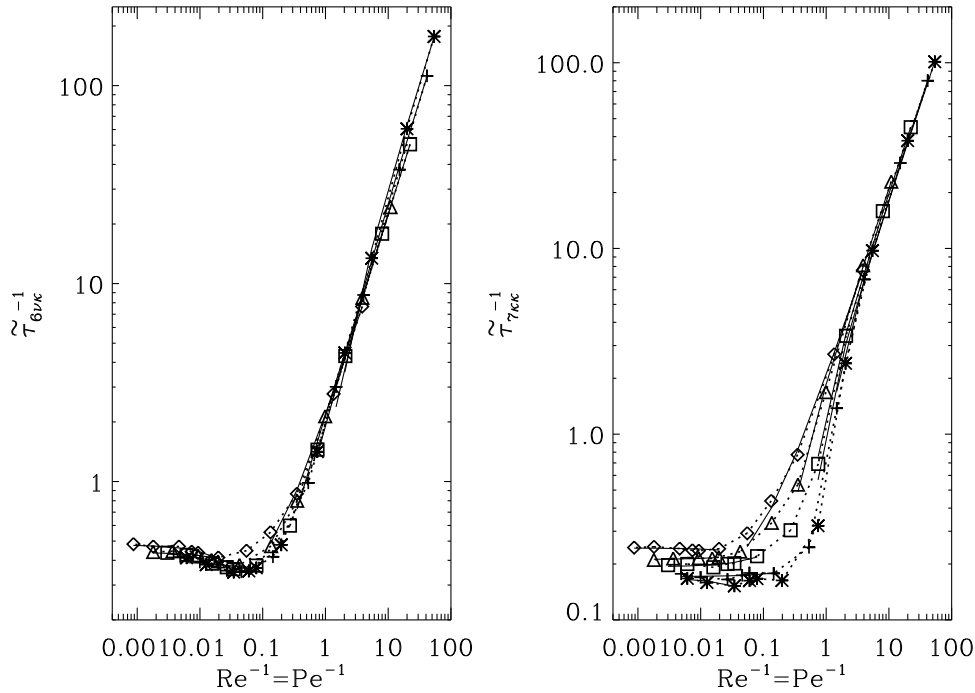


Figure 8. Relaxation times $\tilde{\tau}_{6v\kappa}$ (left) and $\tilde{\tau}_{7\kappa\kappa}$ (right), normalized to the dynamical time τ_0 as functions of $Re^{-1} = Pe^{-1}$, for different values of the scale separation s , indicated at the curves. Dotted lines with symbols: data from method M1; solid lines: linear fits according to (49), separately for low and high Re .

we get

$$\begin{aligned} \frac{\partial \overline{c\nabla h}}{\partial t} = & -c_s^2 \overline{c\nabla\nabla \cdot \mathbf{u}} - \overline{c\nabla(\mathbf{u} \cdot \nabla h)} - \overline{\nabla h \nabla \cdot (\mathbf{u}\overline{C})} \\ & - \overline{\nabla h \cdot \nabla(\mathbf{u}c)}, \end{aligned} \quad (52)$$

$$\begin{aligned} \frac{\partial \overline{(c\nabla h)_i}}{\partial t} = & -\frac{\partial h}{\partial x_i} \frac{\partial u_j}{\partial x_j} \overline{C} - u_j \frac{\partial h}{\partial x_i} \frac{\partial \overline{C}}{\partial x_j} - c_s^2 c \frac{\partial^2 u_j}{\partial x_i \partial x_j} \\ & - \text{third-order terms}, \end{aligned} \quad (53)$$

where the second-order correlation $c \partial^2 u_j / \partial x_i \partial x_j$ can only partly be expressed by $\overline{\mathcal{F}_i}$. Together with the third-order terms, these remaining parts could be modelled by a τ ansatz as used for the diffusion terms in section 2.2, but note that here the ‘diffusivity’ is c_s^2 and we have no argument to consider the not properly modelled terms to be small.

6. Conclusions

The main conclusion to be drawn from this work is that the timescales used to model closure terms in the equations for the mean flux \overline{uc} and the mean square concentration $\overline{c^2}$ are nearly independent of Re for $Re \geq 10$ and also nearly independent of the scale separation ratio for $k_f/k_1 \geq 3$. Expressed in terms of dynamical times, the resulting non-dimensional time scales can be referred to as Strouhal numbers whose values are about 3 for the \overline{uc} closure term and about 7 for the $\overline{c^2}$ closure term. The former value is in good agreement with earlier work using the τ approximation [5]. While it appears that in the statistically stationary regime the model can describe the results of the DNS rather well, we find clear discrepancies in the free decay experiments. There, two different decay rates are detected from which at best one can be explained by the original model. However, when extending the modelling of the triple correlation terms in the equation for $\overline{\mathcal{F}_z}$ to include, apart from the relaxation term, also terms proportional to its

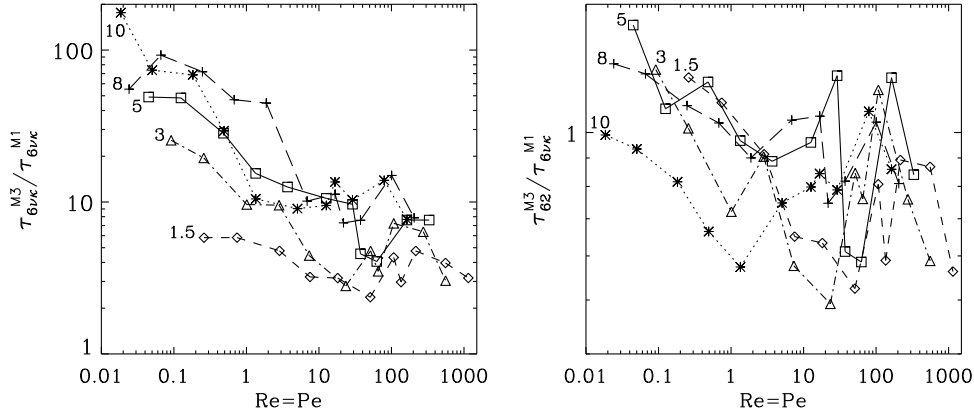


Figure 9. $\tau_{6\nu\kappa}^{M3}/\tau_{6\nu\kappa}^{M1}$ and $\tau_{62}^{M3}/\tau_{6\nu\kappa}^{M1}$, according to (57). Curve labels: scale separation s .

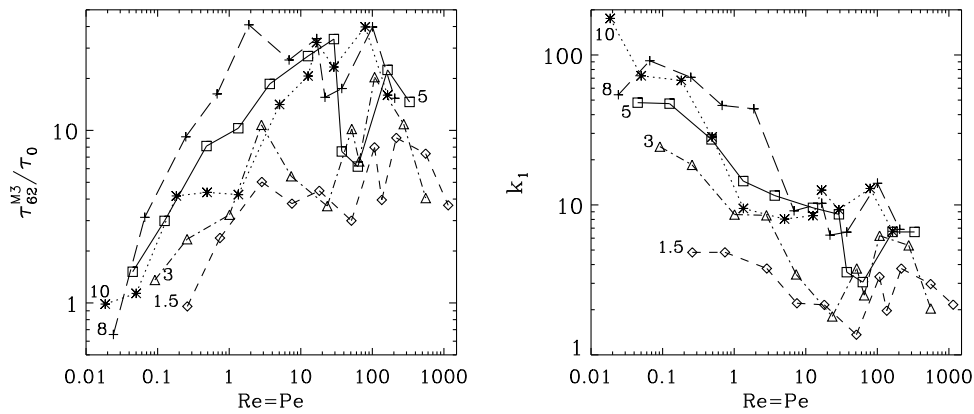


Figure 10. τ_{62} (normalized by τ_0) and k_1 from method M3 according to (60). Curve labels: scale separation s .

first and second time derivatives, consistency with the decay experiments can be achieved.

Equipped with this knowledge, we may now be better justified in using the closure hypotheses discussed here for the quantities \overline{uc} and $\overline{c^2}$. On the other hand, as illustrated by the results of the present study, it is quite clear that these closure hypotheses lack thorough justification [22]. One should therefore in future strive to find systematic discrepancies from the anticipated scalings. One example that we alluded to in this paper is the inhomogeneous case in which the τ approach may break down. Future work in that direction seems now to be highly desirable, because in virtually all astrophysical applications the turbulence is inhomogeneous or at least anisotropic.

Acknowledgments

The authors acknowledge the hospitality of NORDITA during the programme ‘Dynamo, Dynamical Systems and Topology’. We acknowledge the allocation of computing resources by CSC—IT Center for Science Ltd, Espoo, Finland, which is administered by the Finnish Ministry of Education. This work was supported in part by the Finnish Cultural Foundation (JES), the Finnish Academy grants 121431, 136189 (PJK, MR) and 218159, 141017 (MJK), the European Research Council under the AstroDyn Research Project 227952 and

the Swedish Research Council under project 621-2011-5076.

Note added in proof. A basic difficulty of the considered closure is its inability to model the free decay of $\overline{\mathcal{F}}_z$ and $\overline{\mathcal{Q}}$ properly. These processes turned out to require a description by two exponentials with different decay times, see section 4. Including a second order time derivative in modelling the terms on the rhs of (24)

$$\frac{\partial \overline{\mathcal{F}}_z}{\partial t} = -\frac{\overline{\mathcal{F}}_z}{\tau_{6\nu\kappa}} - \tau_{62} \frac{\partial^2 \overline{\mathcal{F}}_z}{\partial t^2} \quad (54)$$

makes resolving this issue possible. With an exponential ansatz for $\overline{\mathcal{F}}_z \propto \exp \lambda t$, the characteristic equation is

$$\lambda^2 + \frac{1}{\tau_{62}} \lambda + \frac{1}{\tau_{6\nu\kappa} \tau_{62}} = 0 \quad (55)$$

having the solution

$$\lambda_{1,2} = -\frac{1}{2\tau_{62}} \left(1 \pm \sqrt{1 - \frac{4\tau_{62}}{\tau_{6\nu\kappa}}} \right). \quad (56)$$

Hence, using $\tau_{6\nu\kappa} > 0$, we have $0 < \tau_{62} < \tau_{6\nu\kappa}/4$ for the observed non-oscillatory decay. The parameters $\tau_{6\nu\kappa}$ and τ_{62} can be derived from the early and late decay times (see

section 4.2.1) by

$$\tau_{6\nu\kappa} = \tau_{6\nu\kappa}^{\text{early}} + \tau_{6\nu\kappa}^{\text{late}}, \quad \tau_{62} = \frac{\tau_{6\nu\kappa}^{\text{early}} \tau_{6\nu\kappa}^{\text{late}}}{\tau_{6\nu\kappa}}, \quad (57)$$

and the results are shown in figure 9. Clearly, the discrepancy in $\tau_{6\nu\kappa}$ between methods M1 and M3 persists.

It can be overcome by using in addition a first-order time derivative when modelling the terms on the rhs of (24):

$$\frac{\partial \bar{\mathcal{F}}_z}{\partial t} = -\frac{\bar{\mathcal{F}}_z}{\tau_{6\nu\kappa}} - k_1 \frac{\partial \bar{\mathcal{F}}_z}{\partial t} - \tau_{62} \frac{\partial^2 \bar{\mathcal{F}}_z}{\partial t^2}. \quad (58)$$

Now the characteristic equation is

$$\lambda^2 + \frac{1+k_1}{\tau_{62}} \lambda + \frac{1}{\tau_{6\nu\kappa} \tau_{62}} = 0 \quad (59)$$

and it is no longer possible to derive all three wanted parameters, $\tau_{6\nu\kappa}$, τ_{62} and k_1 , from the two measured decay times. So we identify $\tau_{6\nu\kappa}$ with the value obtained by method M1, $\tau_{6\nu\kappa}^{\text{M1}}$, and get

$$\tau_{62} = \frac{\tau_{6\nu\kappa}^{\text{early}} \tau_{6\nu\kappa}^{\text{late}}}{\tau_{6\nu\kappa}^{\text{M1}}}, \quad k_1 = \frac{\tau_{6\nu\kappa}^{\text{early}} + \tau_{6\nu\kappa}^{\text{late}}}{\tau_{6\nu\kappa}^{\text{M1}}} - 1. \quad (60)$$

Results are given in figure 10 where it can be seen that the values for the high scale separations $s = 5, 8, 10$ are fairly close to each other. Thus there is most likely an asymptotic for $s \rightarrow \infty$. Note finally the similarity of (58) to (33) (specified for free decay, i.e. $\nabla \bar{C} = \mathbf{0}$).

References

- [1] Blackman E G and Field G B 2002 New dynamical mean-field dynamo theory and closure approach *Phys. Rev. Lett.* **89** 265007
- [2] Blackman E G and Field G B 2003 A new approach to turbulent transport of a mean scalar *Phys. Fluids* **15** L73–L76
- [3] Brandenburg A 2001 The inverse cascade and nonlinear alpha-effect in simulations of isotropic helical hydromagnetic turbulence *Astrophys. J.* **550** 824–40
- [4] Brandenburg A, Haugen N E L and Babkovskaia N 2011 Turbulent front speed in the Fisher equation: dependence on Damköhler number *Phys. Rev. E* **83** 016304
- [5] Brandenburg A, Käpylä P J and Mohammed A 2004 Non-Fickian diffusion and tau approximation from numerical turbulence *Phys. Fluids* **16** 1020–7
- [6] Brandenburg A and Nordlund Å 2011 Astrophysical turbulence modeling *Rep. Prog. Phys.* **74** 046901
- [7] Brandenburg A, Rädler K-H, Rheinhardt M and Käpylä P J 2008 Magnetic diffusivity tensor and dynamo effects in rotating and shearing turbulence *Astrophys. J.* **676** 740–51
- [8] Brandenburg A and Subramanian K 2005 Minimal tau approximation and simulations of the alpha effect *Astron. Astrophys.* **439** 835–43
- [9] Brandenburg A and Subramanian K 2007 Simulations of the anisotropic kinetic and magnetic alpha effects *Astron. Nachr.* **328** 507
- [10] Brandenburg A, Svedin A and Vasil G M 2009 Turbulent diffusion with rotation or magnetic fields *Mon. Not. R. Soc.* **395** 1599–606
- [11] Cattaneo C 1948 On the conduction of heat *Atti Semin. Mat. Fis. Univ. Modena* **3** 83
- [12] Garaud P and Ogilvie G I 2005 A model for the nonlinear dynamics of turbulent shear flows *J. Fluid Mech.* **530** 145–76
- [13] Garaud P, Ogilvie G I, Miller N and Stellmach S 2010 A model of the entropy flux and Reynolds stress in turbulent convection *Mon. Not. R. Astron. Soc.* **407** 2451–67
- [14] Hubbard A and Brandenburg A 2009 Memory effects in turbulent transport *Astrophys. J.* **706** 712–26
- [15] Käpylä P J and Brandenburg A 2008 Lambda effect from forced turbulence simulations *Astron. Astrophys.* **488** 9–23
- [16] Krause F and Rädler K-H 1980 *Mean-Field Magnetohydrodynamics and Dynamo Theory* (Oxford: Pergamon)
- [17] Liljeström A J, Korpi M J, Käpylä P J, Brandenburg A and Lyra W 2009 Turbulent stresses as a function of shear rate in a local disk model *Astron. Nachr.* **330** 92–9
- [18] Madarassy E J M and Brandenburg A 2010 Calibrating passive scalar transport in shear-flow turbulence *Phys. Rev. E* **82** 016304
- [19] Miller N and Garaud P 2007 A practical model of convective dynamics for stellar evolution calculations *AIP Conf. Proc.* **948** 165–9
- [20] Moffatt H K 1978 *Magnetic Field Generation in Electrically Conducting Fluids* (Cambridge: Cambridge University Press)
- [21] Ogilvie G I 2003 On the dynamics of magnetorotational turbulent stresses *Mon. Not. R. Astron. Soc.* **340** 969–82
- [22] Rädler K-H and Rheinhardt M 2007 Mean-field electrodynamics: critical analysis of various analytical approaches to the mean electromotive force *Geophys. Astrophys. Fluid Dyn.* **101** 117–54
- [23] Rheinhardt M and Brandenburg A 2012 Modeling spatio-temporal nonlocality in mean-field dynamos *Astron. Nachr.* **333** 80–6
- [24] Rüdiger G 1989 *Differential rotation and stellar convection Sun and The Solar Stars* (Berlin: Akademie-Verlag)
- [25] Rüdiger G and Hollerbach R 2004 *The Magnetic Universe: Geophysical and Astrophysical Dynamo Theory* (Berlin: Wiley)
- [26] Snellman J E, Brandenburg A, Käpylä P J and Mantere M J 2011 Verification of Reynolds stress parameterizations from simulations *Astron. Nachr.* **332** 883–8
- [27] Snellman J E, Käpylä P J, Korpi M J and Liljeström A J 2009 Reynolds stresses from hydrodynamic turbulence with shear and rotation *Astron. Astrophys.* **505** 955–68